

Stereochemical Influence of the Metal Orbital Occupancy on the Structure of the 1-Sila-3-metallacyclobutane Ring in $(\eta^5\text{-C}_5\text{H}_5)_2\text{M}(\text{CH}_2\text{Si}(\text{CH}_3)_2\text{CH}_2)$, M = Zr, Nb, and Mo

Wayne R. Tikkanen, James W. Egan, Jr., and Jeffrey L. Petersen*

Department of Chemistry, West Virginia University, Morgantown, West Virginia 26506

Received May 1, 1984

X-ray diffraction studies on a series of $(\eta^5\text{-C}_5\text{H}_5)_2\text{M}(\text{CH}_2\text{Si}(\text{CH}_3)_2\text{CH}_2)$ complexes (M = Zr, Nb, and Mo) have been performed to determine the stereochemical influence of the metal's electronic configuration on the conformational structure of the 1-sila-3-metallacyclobutane ring. These three compounds similarly crystallize in a monoclinic unit cell of $P2_1/m$ symmetry with refined lattice parameters. For M = Zr: $a = 8.075$ (1) Å, $b = 11.810$ (5) Å, $c = 15.524$ (4) Å, $\beta = 102.48$ (2)°, $V = 1445.5$ (8) Å³, and $\rho_{\text{calcd}} = 1.417$ g/cm³. For M = Nb: $a = 7.859$ (3) Å, $b = 11.578$ (3) Å, $c = 15.697$ (5) Å, $\beta = 102.74$ (2)°, $V = 1393.3$ (6) Å³, and $\rho_{\text{calcd}} = 1.474$ g/cm³. For M = Mo: $a = 7.627$ (4) Å, $b = 11.395$ (3) Å, $c = 15.874$ (6) Å, $\beta = 102.40$ (3)°, $V = 1347.4$ (7) Å³, and $\rho_{\text{calcd}} = 1.538$ g/cm³. In each case, the crystallographic asymmetric unit consists of two independent molecules that each lie on a crystallographic mirror plane. A comparison of the corresponding structural parameters for molecule 1 in each case reveals that an increase in the number of metal valence electrons from d⁰ Zr(IV) to d¹ Nb(IV) to d² Mo(IV) is manifested by a continual decrease in the C-M-C bond angle from 81.0 (2) to 76.1 (2) to 72.4 (2)° with a gradual increase in the M-C distance from 2.240 (5) to 2.275 (3) to 2.301 (5) Å, respectively. This antibonding influence is further accompanied by a continual increase in the folding of the four-membered MC₂Si ring along the C-C vector from 4.7 to 10.4 to 14.3°, respectively. Full-matrix least-squares refinement (based on F_o^2) converged with respective final discrepancy indices of $R(F_o) = 0.044, 0.034,$ and 0.043 and $\sigma_1 = 1.67, 1.13,$ and 1.90 .

Introduction

During the past decade metallacyclobutanes have developed into an important class of organometallic reagents.¹ Recently, we have reported that the metathetical reaction of $[\text{Mg}(\text{CH}_2)_2\text{Si}(\text{CH}_3)_2]_n$ with a variety of early transition-metal metallocene dihalides affords a convenient synthetic route for a series of 1-sila-3-metallacyclobutane complexes $(\eta^5\text{-C}_5\text{H}_5)_2\text{M}(\text{CH}_2\text{Si}(\text{CH}_3)_2\text{CH}_2)$, M = Ti, Zr, Nb, and Mo.² To date, only the mononuclear structure of $(\eta^5\text{-C}_5\text{H}_5)_2\text{Ti}(\text{CH}_2\text{Si}(\text{CH}_3)_2\text{CH}_2)$ has been confirmed by an X-ray structure determination.² However, the availability of the thermally stable, tetravalent Zr (d⁰), Nb (d¹), and Mo (d²) analogues has provided an opportunity to investigate the stereochemical influence of the metal orbital occupancy on the conformational structure of the 1-sila-3-metallacyclobutane ring. The results of our X-ray diffraction analyses of $(\eta^5\text{-C}_5\text{H}_5)_2\text{M}(\text{CH}_2\text{Si}(\text{CH}_3)_2\text{CH}_2)$, M = Zr, Nb, and Mo, are described herein and provide fundamental structural information about the extent to which the pertinent structural parameters within the MC₂Si ring (i.e., M-C bond distance, C-M-C bond angle, and ring pucker angle) are affected by an alteration of the metal's electronic configuration.

Experimental Section

The 1-sila-3-metallacyclobutane compounds were prepared by previously described methods.² Suitable crystalline samples of $(\eta^5\text{-C}_5\text{H}_5)_2\text{M}(\text{CH}_2\text{Si}(\text{CH}_3)_2\text{CH}_2)$, M = Zr, Nb, and Mo, for the X-ray diffraction analyses were obtained by controlled removal of solvent from a saturated pentane solution of the corresponding metallacycle. To protect them from exposure to air or moisture, the crystals were individually sealed in a glass capillary tube under

a prepurified N₂ atmosphere. These manipulations were performed in a locally constructed dry box³ equipped with an inert-gas purification and recirculation system and a Vacuum-Atmosphere HE-63-P Pedatrol. Each sample was transferred to and optically aligned on a Picker goniostat that is computer controlled by a Krisel Control diffractometer automation system. Analogous procedures⁴ were employed to determine the lattice parameters and to collect the X-ray diffraction data. Each of these three compounds crystallizes in a monoclinic unit cell that is essentially isomorphous with that for $(\eta^5\text{-C}_5\text{H}_5)_2\text{Ti}(\text{CH}_2\text{Si}(\text{CH}_3)_2\text{CH}_2)$.² As a result, the crystallographic asymmetric unit in each case similarly consists of two independent molecules that each lie on a crystallographic mirror plane. Duplicate reflections, previously corrected for absorption⁵ and Lorentz-polarization effects, were averaged. Specific details regarding the lattice parameters and the data collection procedure are summarized in Table I for these three compounds.

The structural analysis was initiated in each case by assigning the positional coordinates for the heavy atom the corresponding values found for the Ti atom in $(\eta^5\text{-C}_5\text{H}_5)_2\text{Ti}(\text{CH}_2\text{Si}(\text{CH}_3)_2\text{CH}_2)$. Subsequent Fourier syntheses provided the approximate coordinates for the remaining non-hydrogen atoms. The positions of the hydrogen atoms for the most part were located from a difference Fourier synthesis that was calculated utilizing only low angle data with $(\sin \theta)/\lambda < 0.40$ Å⁻¹. For the Zr and Mo compounds, idealized coordinates for the methyl hydrogens, however, were calculated by MIRAGE⁶ and included as fixed contributions.

During the structural refinement of $(\eta^5\text{-C}_5\text{H}_5)_2\text{Mo}(\text{CH}_2\text{Si}(\text{CH}_3)_2\text{CH}_2)$, it became evident from the large anisotropic thermal ellipsoids and appreciably shortened C-C bond distances that one of the cyclopentadienyl rings in molecule 1 is disordered. This

(3) Cowie, M., University of Alberta, personal communication.

(4) Jones, S. B.; Petersen, J. L. *Inorg. Chem.* 1981, 20, 2889.

(5) The absorption correction was performed with the use of the general polyhedral shape routine of the program DTALIB. The distance from the crystal center to each face and the appropriate values for the orientation angles (χ and ϕ) to place each face of the rectangular crystal in diffracting position were used to define the crystal's shape, size, and orientation with respect to the laboratory coordinate system of the diffractometer.

(6) Calabrese, J. C. "MIRAGE", Ph.D. Thesis (Appendix), University of Wisconsin—Madison, 1971.

(1) (a) Puddephatt, R. J. *Comments Inorg. Chem.* 1982, 2, 69. (b) Grubbs, R. H. *Prog. Inorg. Chem.* 1978, 24, 1. (c) Calderon, N.; Lawrence, J. P.; Ofstead, E. A. *Adv. Organomet. Chem.* 1979, 17, 449. (d) Katz, T. J. *Adv. Organomet. Chem.* 1977, 16, 283.

(2) Tikkanen, W. R.; Liu, J. Z.; Egan, J. W., Jr.; Petersen, J. L. *Organometallics* 1984, 3, 825.

Table I. Data for the X-ray Diffraction Analyses of $(\eta^5\text{-C}_5\text{H}_5)_2\text{M}(\text{CH}_2\text{Si}(\text{CH}_3)_2\text{CH}_2)$, M = Zr, Nb, and Mo

	Zr	Nb	Mo
A. Crystal Data			
crystal system	monoclinic	monoclinic	monoclinic
space group	$P2_1/m (C_{2h}^2, \text{No. 11})$	$P2_1/m (C_{2h}^2, \text{No. 11})$	$P2_1/m (C_{2h}^2, \text{No. 11})$
a, Å	8.075 (1)	7.859 (3)	7.627 (4)
b, Å	11.810 (5)	11.578 (3)	11.395 (3)
c, Å	15.524 (4)	15.697 (5)	15.874 (6)
β , deg	102.48 (2)	102.74 (2)	102.40 (3)
V, Å ³	1445.5 (8)	1393.3 (6)	1347.4 (7)
fw, amu	307.62	309.31	312.34
d(calcd), g/cm ³	1.417	1.474	1.538
Z	4	4	4
μ , cm ⁻¹	8.03	8.97	10.14
B. Data Collection and Analysis Summary			
cryst dimens, mm	0.625 × 0.50 × 0.125	0.575 × 0.275 × 0.075	0.825 × 0.375 × 0.075
reflectns sampled	$\pm hkl (2\theta = 5-50)$	$\pm hkl (2\theta = 5-50)$	$\pm hkl (2\theta = 5-50)$
2 θ range for centered reflectns, deg	26-35	26-35	27-39
scan rate, deg/min	2	2	2
scan width, deg	1.1 + 0.9 tan θ	1.1 + 0.9 tan θ	1.3 + 0.9 tan θ
no. of standard reflectns	3	3	3
% cryst decay	7	0	4
total no. of measd reflectns	2809	2704	2607
no. of unique data used	2702	2606	2515
agreement between equivalent data			
$R_{\text{av}}(F_o)$	0.024	0.022	0.037
$R_{\text{av}}(F_o^2)$	0.018	0.017	0.064
transmissn coeff	0.707-0.904	0.789-0.938	0.680-0.920
P	0.03	0.03	0.03
discrepancy indices for data with $F_o^2 > \sigma(F_o^2)$			
$R(F_o)$	0.044	0.034	0.043
$R(F_o^2)$	0.054	0.038	0.072
$R_w(F_o^2)$	0.083	0.058	0.086
σ_1 , error in observn of unit wt	1.67	1.13	1.90
no. of variables	218	244	233
data to parameter ratio	13.5:1	10.7:1	11.3:1

disorder is characterized by the fact that C5 (unlike for the Ti, Zr, and Nb analogues) does not reside on a crystallographic mirror plane. This modification follows from a rotation of the cyclopentadienyl ring about its normal such that the angle between the C5-Cp(2) direction, and this mirror plane is ca. 17°. To accommodate this disorder in the structural analysis, idealized coordinates for the ring carbon (C5-C9) and hydrogen (H10-H14) atoms were calculated and refined with isotropic temperature factors. The refinement of the disorder in this manner led to chemically reasonable bond distances and angles for this cyclopentadienyl ring. Full-matrix least-squares refinement⁷⁻¹¹ (based on F_o^2) converged with the corresponding values for the discrepancy indices given in Table I. A final difference Fourier summation verified the completeness of the structural refinement within the limitations of the room temperature data in each case.

The values of the positional parameters for all of the atoms from the last least-squares cycle are provided in Tables II, III, and IV for the Zr, Nb, and Mo compounds, respectively. Selected interatomic distances and angles and their esd's, which were calculated from the estimated standard errors of the fractional coordinates, are summarized in Table V. Tables of the refined thermal parameters, all of the interatomic distances and bond

angles, specific least-squares planes, and the observed and calculated structure factors for $(\eta^5\text{-C}_5\text{H}_5)_2\text{M}(\text{CH}_2\text{Si}(\text{CH}_3)_2\text{CH}_2)$, M = Zr, Nb, and Mo, are available as supplementary material.¹²

Results and Discussion

Description of the Molecular Structure of

$(\eta^5\text{-C}_5\text{H}_5)_2\text{M}(\text{CH}_2\text{Si}(\text{CH}_3)_2\text{CH}_2)$, M = Zr, Nb, and Mo. The mononuclear structures of these 1-sila-3-metalla-cyclobutane compounds have been confirmed by X-ray diffraction methods. The asymmetric unit for each compound similarly contains two independent molecules that each reside on a crystallographic mirror plane. Perspective views for the two $(\eta^5\text{-C}_5\text{H}_5)_2\text{M}(\text{CH}_2\text{Si}(\text{CH}_3)_2\text{CH}_2)$ molecules are illustrated in Figure 1 with the appropriate atom numbering scheme.¹³ For molecule 1 (Figure 1A) the mirror plane passes through the M, Si, MeC1, and MeC2 atoms of the $\text{M}(\text{CH}_2\text{Si}(\text{CH}_3)_2\text{CH}_2)$ fragment and maintains a staggered arrangement for the cyclopentadienyl rings. For molecule 2 (Figure 1B), the mirror plane contains the M, Si, C1, and C2 atoms of the MC_2Si ring and leads to an eclipsed conformation for the symmetry-related cyclopentadienyl ligands. With the exception of the orientation of cyclopentadienyl rings, the structural features

(7) The least-squares refinement⁹ of the X-ray diffraction data was based upon the minimization of $\sum w_i |F_o^2 - S^2 F_c^2|$, where w_i is the individual weighting factor. The discrepancy indices were calculated from the expressions: $R(F_o) = \sum |F_o| - |F_c| / \sum |F_o|$, $R(F_o^2) = \sum |F_o^2 - F_c^2| / \sum F_o^2$, and $R_w(F_o^2) = [\sum w_i |F_o^2 - F_c^2|^2 / \sum w_i F_o^4]^{1/2}$. The standard deviation of an observation of unit weight, σ_1 , equals $[\sum w_i |F_o^2 - F_c^2|^2 / (n - p)]^{1/2}$, where n is the number of observations and p is the number of parameters varied during the last refinement cycle.

(8) The scattering factors employed in all of the structure factor calculations were those of Cromer and Mann⁹ for the non-hydrogen atoms and those of Stewart et al.¹⁰ for the hydrogen atoms with corrections included for anomalous dispersions.¹¹

(9) Cromer, D. T.; Mann, J. *Acta Crystallog., Sect. A* 1968, A24, 231.

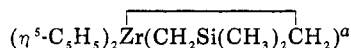
(10) Stewart, R. F.; Davidson, E. R.; Simpson, W. T. *J. Chem. Phys.* 1965, 42, 3175.

(11) Cromer, D. T.; Liberman, D. J. *J. Chem. Phys.* 1970, 53, 1891.

(12) The computer programs that were employed for the X-ray diffraction analyses are described in: Petersen, J. L. *J. Organomet. Chem.* 1979, 155, 179.

(13) Since C5 in molecule 1 in the crystal lattice of $(\eta^5\text{-C}_5\text{H}_5)_2\text{Mo}(\text{CH}_2\text{Si}(\text{CH}_3)_2\text{CH}_2)$ was found not to lie on a crystallographic mirror plane. The numbering scheme for the corresponding atoms in the cyclopentadienyl ring has been modified. The atom numbers in this case were assigned in a counterclockwise manner starting with C5 and H10 through C9 and H14, respectively.

Table II. Positional Parameters for



atom	x	y	z
A. Molecule 1			
Zr	0.45758 (6)	0.2500	0.58935 (3)
Si	0.6348 (2)	0.2500	0.7711 (1)
C1	0.5688 (6)	0.1268 (4)	0.6958 (3)
MeC1	0.5202 (10)	0.2500	0.8628 (5)
MeC2	0.8690 (8)	0.2500	0.8143 (4)
C2	0.1607 (7)	0.2500	0.5008 (5)
C3	0.1738 (5)	0.1547 (5)	0.5539 (4)
C4	0.1919 (5)	0.1928 (4)	0.6406 (4)
C5	0.7389 (12)	0.2500	0.5458 (8)
C6	0.6551 (14)	0.1586 (10)	0.5057 (7)
C7	0.5229 (9)	0.1923 (7)	0.4450 (4)
H1	0.660 (5)	0.090 (3)	0.688 (2)
H2	0.509 (6)	0.079 (4)	0.716 (3)
H3	0.404	0.250	0.848
H4	0.537	0.191	0.901
H5	0.924	0.250	0.767
H6	0.896	0.195	0.844
H7	0.152 (7)	0.250	0.449 (4)
H8	0.176 (6)	0.089 (4)	0.531 (3)
H9	0.203 (6)	0.131 (5)	0.683 (4)
H10	0.805 (13)	0.250	0.577 (7)
H11	0.663 (7)	0.098 (4)	0.518 (4)
H12	0.447 (9)	0.136 (6)	0.414 (5)
B. Molecule 2			
Zr	-0.08148 (6)	0.2500	0.20746 (3)
Si	0.1567 (2)	0.2500	0.0936 (1)
C1	0.2022 (8)	0.2500	0.2178 (4)
C2	-0.0800 (9)	0.2500	0.0625 (4)
MeC	0.2458 (8)	0.1218 (7)	0.0502 (4)
C3	-0.0196 (8)	0.0658 (4)	0.2887 (5)
C4	-0.1550 (7)	0.1118 (4)	0.3144 (4)
C5	-0.2899 (8)	0.1114 (4)	0.2438 (4)
C6	-0.2370 (9)	0.0650 (5)	0.1723 (4)
C7	-0.0694 (10)	0.0376 (5)	0.2003 (5)
H1	0.251 (5)	0.186 (3)	0.243 (3)
H2	-0.128 (5)	0.181 (3)	0.036 (3)
H3	0.211	0.123	-0.001
H4	0.343	0.129	0.064
H5	0.211	0.071	0.072
H6	0.097 (6)	0.067 (4)	0.321 (3)
H7	-0.156 (5)	0.138 (3)	0.371 (3)
H8	-0.391 (6)	0.134 (4)	0.242 (3)
H9	-0.301 (5)	0.052 (4)	0.123 (3)
H10	-0.007 (7)	0.021 (5)	0.176 (4)

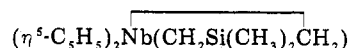
^a The estimated standard deviations in parentheses for this and all subsequent tables refer to the least significant figures.

associated with the two independent molecules in each case are comparable. The ligands adopt a pseudotetrahedral arrangement about the metal that is typical for canted $(\eta^5\text{-C}_5\text{H}_5)_2\text{ML}_2$ -type complexes.

Stereochemical Influence of the Metal Orbital Occupancy.

Although the overall molecular structures of these $(\eta^5\text{-C}_5\text{H}_5)_2\text{M}(\text{CH}_2\text{Si}(\text{CH}_3)_2\text{CH}_2)$ compounds are similar, several significant structural modifications occur as the number of metal valence electrons is increased incrementally from 0 for $\text{M} = \text{Zr}$ to 2 for $\text{M} = \text{Mo}$. Before we can continue with the discussion of our structural data, the effect of the crystallographically imposed mirror symmetry on the determined structural parameters for the two independent molecules in each unit cell must be considered. Although the mirror plane bisects the C1-M-C1' and C1-Si-C1' bond angles in molecule 1, it does not prohibit an accurate determination of the puckering within the MC_2Si ring. In contrast for molecule 2, the mirror plane imposes an artificial planarity for the MC_2Si ring since these four atoms (within the limitations of the room temperature data) appear to lie on the plane. However, upon

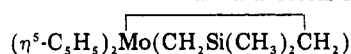
Table III. Positional Parameters for



atom	x	y	z
A. Molecule 1			
Nb	0.44756 (4)	0.2500	0.57989 (2)
Si	0.63376 (17)	0.2500	0.76732 (8)
C1	0.5741 (5)	0.1289 (3)	0.6898 (2)
MeC1	0.5077 (12)	0.2500	0.8558 (5)
MeC2	0.8740 (8)	0.2500	0.8197 (5)
C2	0.1554 (6)	0.2500	0.5004 (4)
C3	0.1738 (4)	0.1524 (3)	0.5547 (3)
C4	0.2005 (4)	0.1907 (3)	0.6406 (3)
C5	0.7241 (8)	0.2500	0.5442 (5)
C6	0.6399 (11)	0.1560 (5)	0.5038 (5)
C7	0.5074 (8)	0.1933 (6)	0.4434 (4)
H1	0.672 (4)	0.093 (3)	0.679 (2)
H2	0.514 (4)	0.076 (3)	0.705 (2)
H3	0.385 (10)	0.250	0.836 (5)
H4	0.530 (7)	0.186 (4)	0.888 (3)
H5	0.940 (7)	0.250	0.775 (4)
H6	0.899 (5)	0.182 (4)	0.850 (3)
H7	0.142 (5)	0.250	0.441 (3)
H8	0.164 (4)	0.078 (3)	0.529 (2)
H9	0.210 (4)	0.145 (3)	0.688 (2)
H10	0.805 (8)	0.250	0.580 (4)
H11	0.660 (5)	0.091 (4)	0.516 (3)
H12	0.438 (8)	0.160 (5)	0.403 (4)
B. Molecule 2			
Nb	-0.08932 (5)	0.2500	0.21207 (2)
Si	0.15599 (18)	0.2500	0.09114 (9)
C1	0.2021 (6)	0.2500	0.2127 (3)
C2	-0.0845 (7)	0.2500	0.0676 (3)
MeC	0.2434 (10)	0.1191 (9)	0.0457 (5)
C3	-0.0183 (6)	0.0747 (3)	0.2931 (3)
C4	-0.1665 (6)	0.1156 (3)	0.3130 (3)
C5	-0.2987 (6)	0.1126 (4)	0.2399 (4)
C6	-0.2331 (8)	0.0680 (4)	0.1731 (4)
C7	-0.0584 (8)	0.0463 (3)	0.2054 (4)
H1	0.260 (4)	0.190 (2)	0.242 (2)
H2	-0.121 (5)	0.179 (3)	0.044 (2)
H3	0.199 (6)	0.124 (4)	-0.004 (3)
H4	0.361 (6)	0.131 (5)	0.067 (3)
H5	0.268 (7)	0.057 (4)	0.081 (3)
H6	0.096 (6)	0.061 (4)	0.334 (3)
H7	-0.188 (5)	0.144 (3)	0.367 (3)
H8	-0.411 (5)	0.139 (4)	0.236 (3)
H9	-0.289 (5)	0.067 (3)	0.126 (2)
H10	0.018 (5)	0.022 (3)	0.186 (2)

closer examination of the size, shape, and orientation of the thermal ellipsoid of the Si atom it becomes evident that the ring is not precisely planar. The maximum root-mean-square thermal displacement for the Si atom in molecule 2 is parallel to the *b* axis and thereby results in a noticeable elongation of the thermal ellipsoid perpendicular to the mirror plane (Figure 1B). Since the X-ray diffraction analysis provides a time-averaged representation of the crystal structure, the refined thermal parameters for the Si atom probably reflect a static disorder that involves the superposition of two symmetry-related puckered structures. This situation arises if the silicon atom is displaced from the MC_2 plane. The plausibility of this description is further supported by the corresponding elongation of the thermal ellipsoid for the unique methyl carbon and by our continual difficulty in trying to find reasonable positions for the methyl hydrogens from low-angle difference Fourier maps. An analysis of the relative magnitudes of the root-mean-square thermal displacements for this Si atom in each case indicates that its thermal ellipsoid could accommodate a displacement ranging from 0.1 to 0.2 Å. Although this disorder appears to be fairly small, it is sufficient to prevent a comprehensive analysis of the structure of the MC_2Si ring in molecule 2. Consequently, any further discussion will focus

Table IV. Positional Parameters for

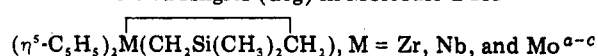


atom	x	y	z
A. Molecule 1			
Mo	0.44303 (6)	0.2500	0.57557 (3)
Si	0.63672 (24)	0.2500	0.76562 (11)
C1	0.5817 (6)	0.1308 (4)	0.6871 (3)
MeC1	0.4993 (11)	0.2500	0.8511 (5)
MeC2	0.8801 (10)	0.2500	0.8232 (5)
C2	0.1587 (8)	0.2500	0.5045 (5)
C3	0.1793 (5)	0.1487 (4)	0.5579 (3)
C4	0.2109 (5)	0.1887 (4)	0.6440 (3)
C5	0.7201 (11)	0.2196 (7)	0.5420 (6)
C6	0.5917 (17)	0.1469 (9)	0.4895 (8)
C7	0.4715 (12)	0.2213 (8)	0.4362 (6)
C8	0.5216 (15)	0.3370 (10)	0.4542 (7)
C9	0.6732 (14)	0.3399 (9)	0.5194 (6)
H1	0.670 (6)	0.100 (4)	0.677 (3)
H2	0.518 (6)	0.076 (4)	0.695 (3)
H3	0.383	0.250	0.825
H4	0.523	0.182	0.882
H5	0.967	0.250	0.782
H6	0.908	0.183	0.853
H7	0.117 (7)	0.250	0.442 (3)
H8	0.165 (5)	0.066 (4)	0.537 (3)
H9	0.235 (5)	0.136 (3)	0.694 (2)
H10	0.790 (9)	0.212 (6)	0.582 (4)
H11	0.593 (10)	0.073 (6)	0.490 (5)
H12	0.395 (9)	0.206 (6)	0.393 (5)
H13	0.491 (12)	0.411 (9)	0.436 (6)
H14	0.722 (10)	0.410 (7)	0.544 (5)
B. Molecule 2			
Mo	-0.08764 (6)	0.2500	0.21841 (3)
Si	0.15995 (26)	0.2500	0.09018 (12)
C1	0.2094 (8)	0.2500	0.2089 (4)
C2	-0.0877 (11)	0.2500	0.0722 (5)
MeC	0.2463 (10)	0.1189 (8)	0.0425 (4)
C3	-0.0149 (8)	0.0881 (4)	0.3027 (4)
C4	-0.1774 (10)	0.1230 (5)	0.3112 (5)
C5	-0.2983 (9)	0.1131 (6)	0.2362 (8)
C6	-0.2077 (16)	0.0666 (7)	0.1761 (6)
C7	-0.0328 (11)	0.0539 (5)	0.2178 (5)
H1	0.269 (6)	0.186 (4)	0.240 (3)
H2	-0.123 (9)	0.180 (6)	0.060 (5)
H3	0.196	0.123	-0.010
H4	0.360	0.132	0.053
H5	0.217	0.063	0.070
H6	0.095 (8)	0.082 (5)	0.351 (4)
H7	-0.220 (9)	0.159 (6)	0.368 (4)
H8	-0.420 (12)	0.142 (7)	0.227 (6)
H9	-0.250 (10)	0.066 (7)	0.137 (4)
H10	0.050 (7)	0.033 (5)	0.205 (3)

primarily on a comparison of the pertinent structural parameters obtained for molecule 1, which are summarized in Table V for $(\eta^5\text{-C}_5\text{H}_5)_2\text{M}(\text{CH}_2\text{Si}(\text{CH}_3)_2\text{CH}_2)$, $\text{M} = \text{Zr}$, Nb , and Mo .

The basis for our analysis relies on a qualitative molecular orbital description developed by Lauher and Hoffmann¹⁴ to describe the bonding in $(\eta^5\text{-C}_5\text{H}_5)_2\text{ML}_2$ -type complexes. As the two cyclopentadienyl rings about a $(\eta^5\text{-C}_5\text{H}_5)_2\text{M}$ molecular fragment move from a parallel to a canted arrangement, three metal orbitals ($1a_1$, b_2 , and $2a_1$ under C_{2v} symmetry) become available to accept electrons from the donor ligand orbitals. For these 1-sila-3-metallacyclobutane complexes, the two M-C bonds within the four-membered ring arise from the σ donation of the electron pairs from the corresponding a_1 and b_2 orbitals of the $[\text{CH}_2\text{Si}(\text{CH}_3)_2\text{CH}_2]^{2-}$ dianion into the appropriate metal orbitals. These bonding interactions result in placing the nonbonding $1a_1$ orbital above the two filled

Table V. Pertinent Interatomic Separations (Å) and Bond Angles (deg) in Molecule 1 for



	Zr	Nb	Mo
A. Interatomic Separations			
M-C1	2.240 (5)	2.275 (3)	2.301 (5)
C1-Si	1.870 (5)	1.848 (4)	1.831 (5)
Si-MeC1	1.858 (9)	1.876 (10)	1.884 (9)
Si-MeC2	1.865 (6)	1.886 (6)	1.885 (7)
M-Cp(1)	2.223 (4)	2.093 (3)	1.969 (5)
M-Cp(2)	2.231 (11)	2.094 (8)	1.992 (12)
M...Si	2.875 (2)	2.983 (1)	3.061 (2)
C1...C1'	2.868 (9)	2.804 (7)	2.718 (9)
B. Bond Angles			
C1-M-C1'	81.0 (2)	76.1 (2)	72.4 (2)
Cp(1)-M-Cp(2)	132.8 (2)	136.9 (2)	140.0 (3)
M-C1-Si	88.3 (2)	92.1 (1)	94.9 (2)
C1-Si-C1'	102.2 (3)	98.7 (2)	95.8 (3)
MeC1-Si-MeC2	111.0 (3)	108.6 (3)	107.1 (3)
θ , folding angle	4.7	10.4	14.3

^a Cp(*n*) denotes cyclopentadienyl ring centroid.

^b Prime (') denotes the symmetry-related atom on opposite side of crystallographic mirror plane passing through M, Si, MeC1, and MeC2 of molecule 1. ^c The esd's for the interatomic distances and bond angles were calculated from the standard errors of the fractional coordinates of the corresponding atomic positions.

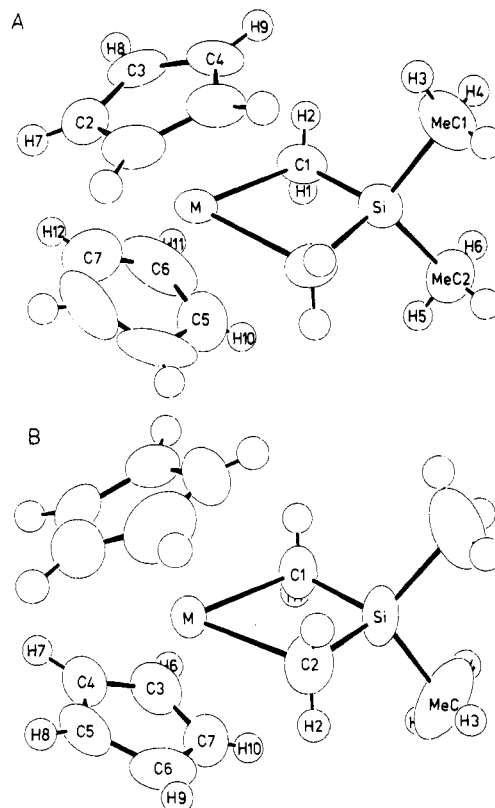


Figure 1. Perspective views of the molecular configurations of the two $(\eta^5\text{-C}_5\text{H}_5)_2\text{M}(\text{CH}_2\text{Si}(\text{CH}_3)_2\text{CH}_2)$ molecules ($\text{M} = \text{Zr}$, Nb , Mo) with the appropriate numbering scheme¹³ for molecule 1 (A) and molecule 2 (B), respectively. The thermal ellipsoids are scaled to enclose 50% probability, and the radii of the spheres for the hydrogen atoms were arbitrarily reduced for clarity.

bonding levels. The metal orbital character and the spatial orientation of this metal-based a_1 orbital have been examined by dilute single-crystal EPR studies of $(\eta^5\text{-C}_5\text{H}_4\text{CH}_3)_2\text{MCl}_2$ ($\text{M} = \text{V}$,¹⁵ Nb ¹⁶). For these structurally

similar d^1 paramagnetic compounds the unpaired electron resides in an orbital of mainly d_{z^2} character with a small admixture of $d_{x^2-y^2}$. This d_{z^2} -like orbital is directed normal to the plane which bisects the Cl-M-Cl bond angle and is antibonding with respect to those ligands that possess high-lying π -donor orbitals, such as halide. Consequently, as this a_1 orbital is occupied, structural studies of first-¹⁵ and second-row¹⁷ metallocene dichloride complexes have shown that this antibonding influence is manifested by a significant lengthening of the M-Cl bond and is accompanied by a concomitant reduction of the Cl-M-Cl bond angle.

An examination of the structural data in Table V reveals that analogous trends are observed for the M-C bond distance and the C-M-C bond angle in $(\eta^5\text{-C}_5\text{H}_5)_2\text{M}(\text{CH}_2\text{Si}(\text{CH}_3)_2\text{CH}_2)$, M = Zr, Nb, and Mo. As one progresses from the d^0 Zr(IV) to the d^2 Mo(IV) compound, we observe a continual increase in the M-C bond distance from 2.240 (5) to 2.301 (5) Å. Although this elongation of the M-C bond may appear to be relatively small, its significance is more adequately demonstrated by the consideration of the corresponding large decrease associated with the average M-Cp(*n*) distances. The ca. 0.25-Å difference between the average Zr-Cp(*n*) and Mo-Cp(*n*) distances of 2.227 and 1.981 Å, respectively, is consistent with the reduction of the metal's covalent radius as one proceeds from Zr to Mo. A comparable decrease for the M-Cp(*n*) distances has been reported for $(\eta^5\text{-C}_5\text{H}_5)_2\text{MCl}_2$, M = Zr, Nb, and Mo.¹⁷ Upon taking this into account, the Nb-C and Mo-C separations within the corresponding 1-sila-3-metallacyclobutane rings are actually ca. 0.16 and 0.31 Å longer than the corresponding bond distances predicted solely on the basis of covalent radii considerations. Since the bonding mode of the $[\text{CH}_2\text{Si}(\text{CH}_3)_2\text{CH}_2]^{2-}$ ligand does not involve a π -donor contribution, an alternative explanation for this antibonding effect is needed. One possibility is that its origin arises from the reduction of the σ -bonding contribution from the metal's $2a_1$ orbital, which becomes rehybridized upon occupation of the previously unoccupied $1a_1$ orbital.

In addition to its antibonding influence with regard to the M-C bonds, an increase in the orbital occupancy of this metal-based orbital produces several other stereochemical modifications within the MC_2Si ring. The C-M-C bond angle progressively decreases from 81.0 (2)° for M = Zr to 76.1 (2)° for M = Nb to 72.4 (2)° for M = Mo in $(\eta^5\text{-C}_5\text{H}_5)_2\text{M}(\text{CH}_2\text{Si}(\text{CH}_3)_2\text{CH}_2)$. This trend is consistent with the expected spatial orientation of the $1a_1$ orbital with respect to the MC_2Si ring. The reduction of this angle is further accompanied by comparable decreases and increases in the C1-Si-C1' and M-C1-Si bond angles, respectively. Presumably, the ring strain introduced by the reduction of the C1-M-C1' bond angle is relieved in part by an appropriate increase in the puckering of the ring. The folding angle, θ , of the MC_2Si ring about the C1...C1' vector in $(\eta^5\text{-C}_5\text{H}_5)_2\text{M}(\text{CH}_2\text{Si}(\text{CH}_3)_2\text{CH}_2)$ is 4.7°, 10.4°, and 14.3° for M = Zr, Nb, and Mo, respectively. The reduction of the C-M-C bond angle is also accompanied

by a noticeable increase in the Cp(1)-M-Cp(2) angle (132.8 (2)° for M = Zr; 136.9 (2)° for M = Nb; 140.0 (3)° for M = Mo) for the nearly staggered conformation of the cyclopentadienyl rings in molecule 1. Although this increase could be attributed to interring repulsions that are introduced as the metal's size decreases, it is somewhat surprising to find that the same general trend is observed for molecule 2 in which the rings remain in the sterically more-hindered eclipsed conformation. Consequently, inter-ring repulsions appear to play a relatively minor role in dictating the conformational structure of the cyclopentadienyl rings in these $(\eta^5\text{-C}_5\text{H}_5)_2\text{M}(\text{CH}_2\text{Si}(\text{CH}_3)_2\text{CH}_2)$ compounds. Alternatively, the reduction of C1-M-C1' bond angle helps to alleviate steric interactions between the $\text{M}(\text{CH}_2\text{Si}(\text{CH}_3)_2\text{CH}_2)$ and the cyclopentadienyl rings and leads to some rehybridization of the metal valence orbitals. These factors collectively allow the cyclopentadienyl rings to attain a more parallel orientation as reflected by the observed increase in the corresponding Cp(1)-M-Cp(2) angle.

Concluding Remarks

The stereochemical information provided by our structural studies of $(\eta^5\text{-C}_5\text{H}_5)_2\text{M}(\text{CH}_2\text{Si}(\text{CH}_3)_2\text{CH}_2)$, M = Zr, Nb, and Mo, has shown the metal's electronic configuration exhibits a significant influence upon the M-C bond distance, the C-M-C bond angle, and the puckering of the MC_2Si ring. Although the corresponding metallacyclobutane compounds of these metals remain to be prepared and structurally characterized, the structural trends observed here presumably are directly applicable to these metallacyclobutane analogues as well. More importantly, the antibonding influence introduced by the occupancy of the metal's a_1 orbital on the M-C bond in these 1-sila-3-metallacyclobutane complexes provides some insight into the initial structural alterations that precede the insertion of a nucleophile into the M-C bond of an electron-deficient, four-membered metallacycle such as $(\eta^5\text{-C}_5\text{H}_5)_2\text{Zr}(\text{CH}_2\text{Si}(\text{CH}_3)_2\text{CH}_2)$. Our structural data qualitatively suggest that electron donation into the metal's empty d_{z^2} -like orbital should be accompanied by a simultaneous lengthening (weakening) of the Zr-C bonds and thereby makes them more susceptible to insertion. Efforts are in progress to determine the extent that the electron-deficient character of the d^0 Zr(IV) center can be utilized to induce and direct the insertion of various nucleophiles into the Zr-C bonds of this 1-sila-3-zirconacyclobutane compound.

Acknowledgment. We wish to thank the National Science Foundation Grant No. ISP-8011453 for financial support of this research. Computer time for the analysis of the X-ray diffraction data was generously provided by the West Virginia Network for Educational Telecomputing.

Registry No. $(\eta^5\text{-C}_5\text{H}_5)_2\text{Zr}(\text{CH}_2\text{Si}(\text{CH}_3)_2\text{CH}_2)$, 89530-31-4; $(\eta^5\text{-C}_5\text{H}_5)_2\text{Nb}(\text{CH}_2\text{Si}(\text{CH}_3)_2\text{CH}_2)$, 89530-32-5; $(\eta^5\text{-C}_5\text{H}_5)_2\text{Mo}(\text{CH}_2\text{Si}(\text{CH}_3)_2\text{CH}_2)$, 89530-33-6.

Supplementary Material Available: Tables of refined thermal parameters, all of the bond distances and angles, least-squares planes, and observed and calculated structure factors (39 pages). Ordering information is given on any current masthead page.

(16) Petersen, J. L.; Egan, J. W., Jr. *Inorg. Chem.* 1983, 22, 3571.

(17) Prout, K.; Cameron, T. S.; Forder, R. A.; Critchley, S. R.; Denton, B.; Rees, G. V. *Acta Crystallogr. Sect. B* 1974, B30, 2290 and references cited therein.